A comparative study on Co(II) removal capacity from water samples by sorption using limestone and nanolimestone

Ahmed H. Elmorsy, Mohamed EL-Toony, Enas Al-Johani and Shamha Ghurzan

ABSTRACT

Powdered nanolimestone (NLS) and limestone (LS) have been investigated as an adsorbent for the removal of cobalt from aqueous solutions. Batch experiments were carried out to investigate the effect of pH. The favorable pH for maximum cobalt adsorption was 6.8. The surface area increased in the case of NLS up to 6.2 m^2/g, while it was equal to 0.5 m^2/g in the case of LS. The adsorption capacity calculated by the Langmuir equation was 17.1 mg/g for LS and 60.0 mg/g for NLS at pH 6.8. The adsorption capacity increased with temperature and the kinetics followed a first-order rate equation. The enthalpy change (ΔH^o) was 20.8 $Jmol^{-1}$ for LS and 41.6 $Jmol^{-1}$ for NLS, while entropy change (ΔS^o) was 33.3 JK^{-1} mol^{-1} for LS and 74.8 JK^{-1} mol^{-1} for NLS, which substantiates the endothermic and spontaneous nature of the cobalt adsorption process. All of the results suggested that the NLS is very strong and could be an excellent nano-adsorbent for cobalt contaminated water treatment more than limestone.

Key words | adsorption, cobalt, kinetics, nanolimestone, thermodynamic

Ahmed H. Elmorsy (corresponding author)
Mohamed EL-Toony
Department of Chemistry, College of Science,
King Khalid University,
Tehama 900,
Saudi Arabia
E-mail: *ahrejab@kku.edu.sa*

Enas Al-Johani
Department of Chemistry, College of Science,
Majmaah University,
Majmaah 11952,
Saudi Arabia

Shamha Ghurzan
Department of Chemistry, College of Science,
Najran University,
Najran,
Saudi Arabia

INTRODUCTION

Cobalt(II) ion is a toxic heavy metal ion in industrial wastewater. A trace amount ($\mu g L^{-1}$) of cobalt is required and necessary for some organisms as a cofactor for enzymatic activities. However, for most of organisms, concentrations at ppm (5 mg L^{-1}) level are known to be toxic because of the irreversible inhibition of some enzymes by heavy metal ions (Leyssens *et al.* 2017). In humans, cobalt deficiency has never been reported, but the toxic effects of excess cobalt have been fully described as excess intake will cause acute poisoning by mouth in humans producing gastrointestinal upsets, and chronic absorption may cause abnormalities in skin, heart, blood, or lungs (Payne 1977).

Due to the mobility and toxicity in natural water ecosystems, the presence of Co(II) ions in surface water and groundwater poses a major inorganic contamination problem. To date, there are various technologies for removing heavy metal ions from solution, including filtration, surface complexation, chemical precipitation, ion exchange, adsorption, electrode position, and membrane processing (Al-Qodah 2006).

Most of these processes are unacceptable owing to their high cost, low efficiency, disposal of sludge, and inapplicability to a wide range of pollutants (Quintelas *et al.* 2009). Adsorption, on the other hand, is one of the most recommended physico-chemical treatment processes that is commonly used and applied for heavy metals' removal from water samples and aqueous solutions. In addition, the adsorption process is well recognized as one of the

doi: 10.2166/wrd.2019.060

most efficient methods for removal of heavy metals from their matrices. Adsorption is mainly based on the utilization of solid adsorbents from either organic, inorganic, biological, or low cost materials (Camel 2003). Heavy metal removal via adsorption by organic adsorbents is usually accomplished by the application of polymeric ion-exchangers in which the binding and interaction of metal species with these adsorbents is favored via ion-exchange mechanism, or by application of chelating polymers where the target metal ions are directly attached to the adsorbents via chelating or complex formation mechanism (Gode & Pehlivan 2003). Naturally occurring materials, either modified or unmodified, organic adsorbents such as chitosan and cross-linked carboxymethyl-chitosan (Sun & Wang 2006), polysaccharide-based materials, and lignocellulosic fibers with their surface characteristic functional groups in the form of hydroxyl or carboxyl have also been of great research interest. Biological adsorbents, referred to as biosorbents, are commonly derived from biological components such as bacteria, fungi, and algae, that are characterized and capable of complex formation and/or ion-exchange reactions with metal ions via their functional groups in a process known as biosorption (Abdel-Raouf & Abdul-Raheim 2017).

Removal and extraction of heavy metals based on applications of biosorption approach are commonly performed owing to the major advantages of various biosorbents, such as economical nature, eco-friendly behavior, regeneration for multiple uses, and high selectivity towards different metals (Quintelas *et al.* 2009; Singh *et al.* 2017). Low cost adsorbent materials originating from industrial products or wastes are also known as biosorbents and are widely used for the removal of heavy metals from water samples, and these include components of plants, wood, grasses, compost, peat moss, and carbon materials (Romero-Gonzalez *et al.* 2006).

Inorganic solid adsorbents such as novel silica gel matrix (Elkady *et al.* 2016), alumina with immobilized 1-nitroso-2-naphthol (Reshetnyak *et al.* 2012), nano-TiO_2 (Mohammadi & Aliakbarzadeh Karimi 2017), and bentonite adsorbent (Ndifor-Angwafor *et al.* 2017) are well characterized by their high mechanical properties and strong resistivity to thermal degradation as compared to other biosorbents or organic adsorbents.

In recent years, there has been interest in discovering new products that have minimal environmental impact for restoration or remediation of natural resources (Quintelas *et al.* 2009).

Limestone (LS) which is produced in large quantities in many countries (among them Egypt) is a low-cost reactive medium that can be used for the retaining of heavy metals and the subsequent clean-up of industrial effluents, leachates, and contaminated ground water (Aziz *et al.* 2008). Hence, the objective of the present work was to study the possibility of utilizing LS (which is naturally occurring or readily available and cheap) as a sorbent for removing cobalt ions from aqueous solutions and natural waters. The different parameters influencing the adsorption of cobalt ions onto powdered limestone were optimized and the results are presented in this work.

INSTRUMENTAL STUDIES

The difference between nanolimestone (NLS) and LS is interpreted as a term of results of XRD and SEM analysis (JSM 6510 LV). Powered XRD (MiniFlex, HyPix-400 MF) studies help to understand the changes occurring in the surface morphologies for the two sorbents. The XRD patterns of LS and NLS (Figure 1) show almost no change in the Lin (counts) for the peak at 2θ which is indicated by the fact that neither has any change of calcium content. In the SEM images of LS and NLS (Figure 2), responding to the morphological changes in the surface of the adsorbents in the coverage of pores with a high porosity for NLS, and the surface deformation, may indicate the incorporation of the metal ion particles into NLS pores.

EXPERIMENTAL

Samples

The limestone (LS), $CaCO_3$ samples used in this study were obtained from the Al-Mokattam area in Cairo (Egypt) where some private and governorate quarries

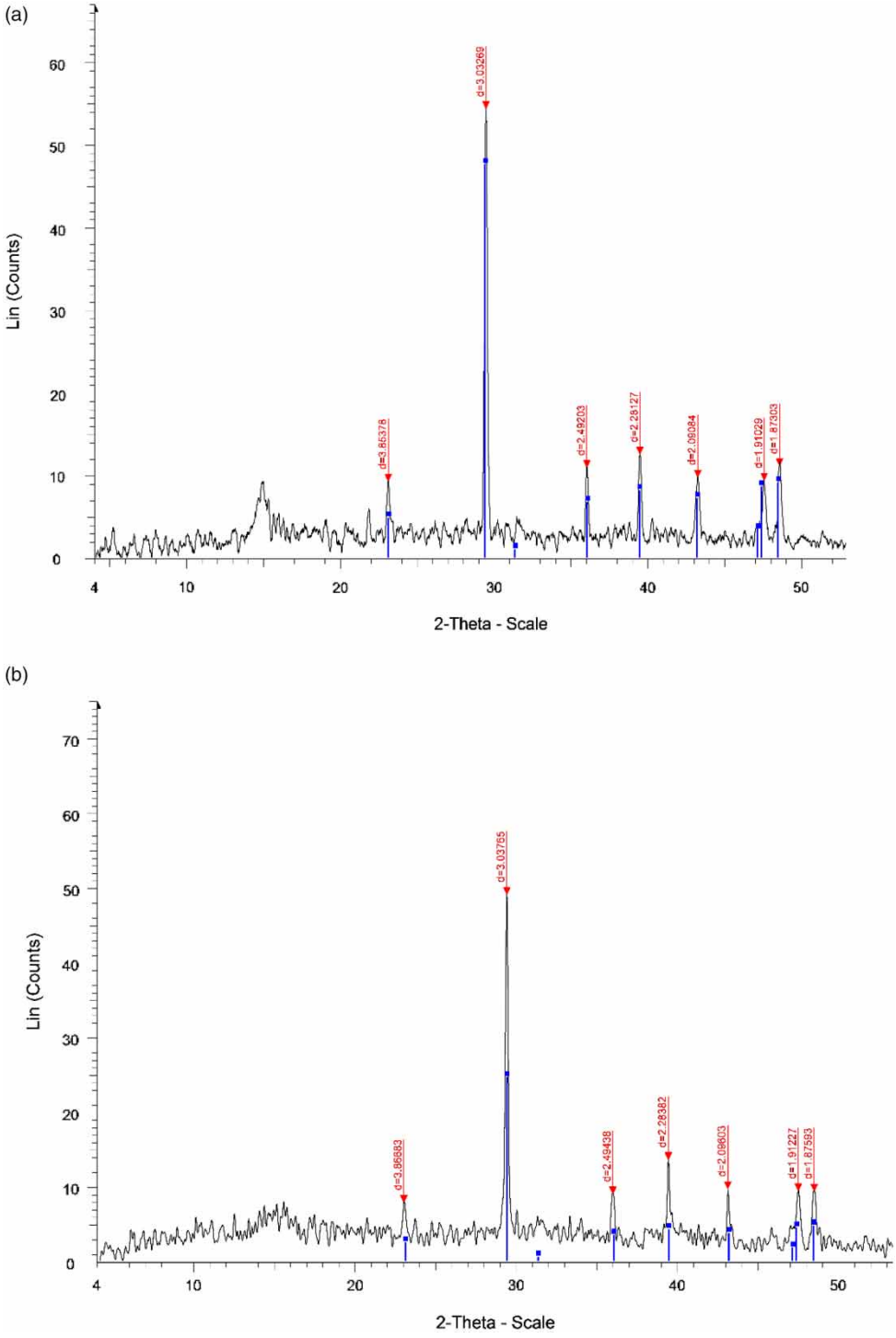

Figure 1 | (a) XRD for LS and (b) XRD for NLS.

are located. The samples were crushed and pulverized in the laboratory and those with a mean size of ca. 12.5 mm were used in the experiments.

The samples contained 92% calcite and 3% dolomite (as found by elemental chemical analyzer 2400 Series II, Perkin-Elmer) as has been previously described (Aziz *et al.*

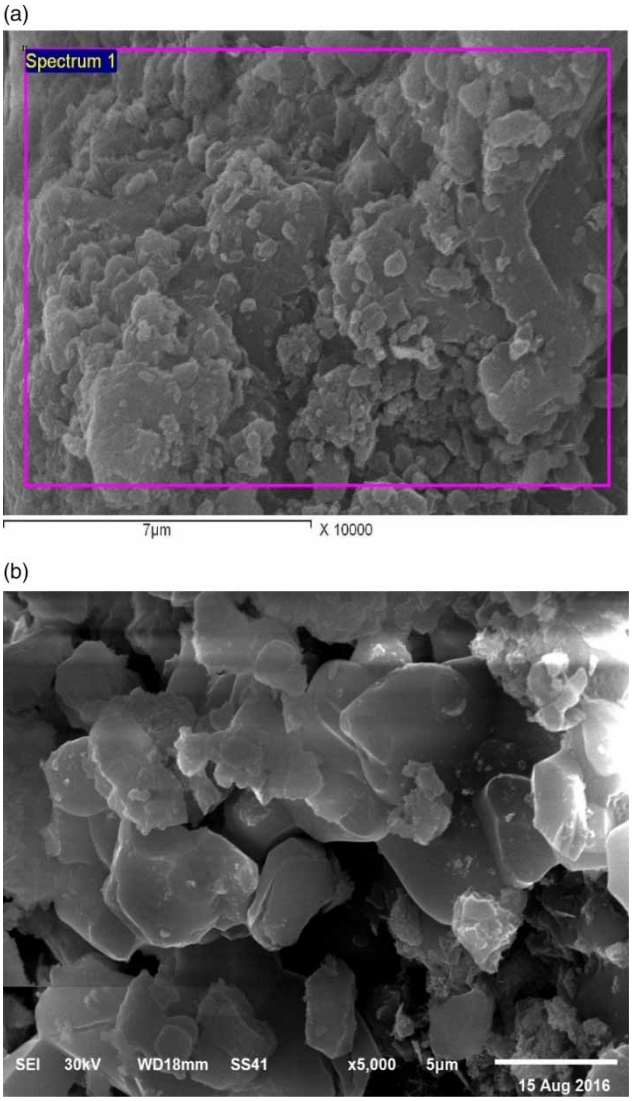

Figure 2 | (a) SEM for LS and (b) SEM for NLS.

2008) The remainder of the samples was composed of common minor constituents such as silica, clay, feldspar, pyrite, and sedrite (Bates & Jackson 1980). The samples were dried for 2 h in an oven at 125 °C, packed into stoppered bottles, and stored in a desiccator for future use. Functional groups of LS were characterized through infrared analysis.

The LS spectrum coincided with pure $CaCO_3$. The surface area and porosity of NLS/LS was measured using the Brunauer, Emmett and Teller (BET) method (Quantachrome TouchWin). LS presented no BET porosity and its measured surface area was 0.50 $m^2 g^{-1}$ for limestone and 6.2 $m^2 g^{-1}$ for nanolimestone. The pH values of points of zero charge (pHPZC) using a Zetasizer Nano ZSP (Malvern Panalytical) were 9.1 (not aged), 6.2 (aged 60 min) and 8.3 (aged several days), and this agreed with previously reported data (Somasundaran & Goddard 1979). Stirring the LS and NLS sorbent with distilled water (pH = 6.8) for 1 h decreases the suspension pH to 5.8, confirming the positive charge of the LS and NLS surfaces. Also, the concentration of calcium ion in the solution was measured before and after adsorption in order to confirm that cation exchange was involved.

Reagents

All the solutions were prepared from certified reagent grade chemicals. A cobalt chloride stock solution of 1 molar concentration was prepared and the working solutions were made by diluting the former with doubly distilled water. Aqueous solutions of HNO_3 and NaOH were used for pH adjustments.

Nanolimestone was prepared by dissolving the powdered limestone in about 150 g of concentrated HCl. The obtained calcium chloride solution was mixed with 1.5 g of chitosan, which was dissolved in 3% acetic acid. This mixture was blended with 70 g Na_2CO_3 and slightly heated to complete the reaction. The mixture was kept overnight, then filtered and washed several times with water. Finally, it was calcined in a muffle furnace at 650 °C for 2 hr (Hariharan *et al.* 2014).

Procedure

Unless stated otherwise, all batch sorption experiments were conducted at room temperature (ca. 25 °C). Known volumes of Co(II) ions solutions with concentrations ranging from 2 to 100 mg/L were pipetted into quick-fit glass bottles containing 0.1 g of NLS sorbent or 1 g of LS in 100 mL aqueous solution. Since the pH of any of the resulting solutions was about 7.0, no further control was necessary since it was suitable for most adsorption experiments. The resulting solutions were then stirred with a magnetic stirrer at 250 rpm and the samples were taken at fixed time periods (0.0, 0.3, 0.8, 1.0 5.0, 10, 20, 30, 60, and 90 min) in order to study the kinetics of the adsorption

process. Preliminary experiments showed that this time length was sufficient for adsorption of Co(II) ions onto NLS or LS. The samples were subsequently filtered off and the residual Co(II) ions concentrations in the filtrate were analyzed using atomic absorption spectroscopy (AAS). Also, the candidate can be reused again in the industrial field (Aliabdo *et al.* 2014).

Experimental data analysis

The percentage adsorption of Co(II) ion from the solution was calculated from the relationship:

$$\%Adsorption = (C_i - C_f)/C_i \times 100 \quad (1)$$

where C_i corresponds to the initial concentration of Co(II) ion and C_f is the residual concentration after equilibration. The metal uptake q (mg/g) was calculated as:

$$q = [(C_i - C_f)/m].V \quad (2)$$

where m is the quantity of sorbent (mg) and V the volume of the suspension (mL).

RESULTS AND DISCUSSION

Effect of pH

The pH value of the solution plays an important role in the sorption of Co(II) ions on LS or NLS. The sorption of Co(II) ions to LS increases from ~20% to ~90% in the pH ranging from 4 to 7 and then maintains a high level with increasing pH values (see Figure 3). Similar results were also reported for Cu(II) sorption to TiO_2 (Kim *et al.* 2003).

The pH values of the solution after sorption equilibrium changes a little to the acidic region, which indicates that H^+ is released during the sorption process. In aqueous systems, the surface groups of sorbent can be protonated in different extents. Therefore, the concentrations of surface species of the sorbent change under different pH values. With increasing pH, the negative charged groups or deprotonated groups increase and the hydrolysis of Co(II) also increases. As can

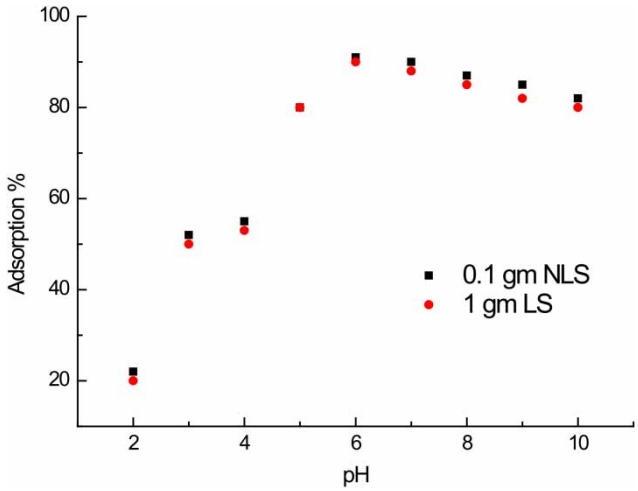

Figure 3 | Adsorption (%) of Co(II) ions (6 mg.L^{-1}) by NLS/LS vs. pH.

be seen, below pH 2, the removal of Co(II) ions reaches zero which may be attributed to the complete solubility of LS (consists mainly of $CaCO_3$ and $MgCO_3$), thereby hindering the sorption of cobalt ions. Above pH 2, the removal efficiency increases, reaching a maximum value (ca. ~90%) over the pH range 6–7 followed by a decrease.

The removal of the Co(II) ions at pH value 5 may be attributed to a possible ion-exchange mechanism between Co(II) ions and calcium containing LS in a similar manner to that reported by Hussain & Ivanovic (2015). Also, this was confirmed by measuring the concentration of calcium ion in the solution before and after adsorption where its value was increased. Adsorbed Co(II) ions generally occupy calcium sites within the calcite lattice (Cherniak 1997). The enhanced removal of metal ion as the solution pH is increased (more than 5) can be attributed to adsorption of hydrolytic product $Co(OH)^+$ (Ghazy & Ragab 2007), and/or surface precipitation of the metal as the insoluble carbonates, $CoCO_3$, form successive layers on the sorbent surface, which may be explained in the following equations (Apak *et al.* 1998):

$$= CaCO_3^o + M^{2+} + HCO_3^- = MCO_3^o + H^+ \quad (3)$$

$$= MCO_3^o + M^{2+} + HCO_3^- = MCO_3^o + H^+ \quad (4)$$

The decrease in the removal efficiency at high pH values may be attributed to the fact that the negative species of

cobalt, $Co(OH)_3^-$ and $Co(OH)_4^{2-}$, are not capable of a combination with the negative surface of LS, as determined by ZPC ($pH_{ZPC} = 6.2$ after which the surface is negative). Moreover, this finding was confirmed by stirring NLS or LS with distilled water; the pH of the suspension was always decreased from 6.8 to 5.8. Therefore, pH 7 was recommended throughout all the other experiments.

Sorption model

Adsorption kinetics is one of the most important characteristics representing adsorption efficiency. The adsorption rate of cobalt adsorption on the LS surface, as a function of the initial cobalt concentration, is shown in Figure 4. Due to faster adsorption kinetics with smaller particles (Badruzzaman *et al.* 2004), the cobalt adsorption was initially rapid, after which it decreased.

The time required to reach equilibrium was 60 min for all cobalt concentrations. The initial rapid adsorption was presumably due to electrostatic attraction. The slow adsorption in the later stage represented a gradual uptake of fluoride at the inner surface by complexation or ion-exchange or due to the decrease in the number of adsorption sites having affinity toward cobalt(II) ions (Sapuan *et al.* 2013).

A standard parameter was used for studying the behavior of the metal adsorption onto the adsorption surface, 50 mg.L^{-1} of the Co(II) ions adsorbent on LS and NLS surface using the Morris-Weber equation (Doğan *et al.* 2004):

$$q = K_d(t)^{1/2} \tag{5}$$

where q is the amount of Co(II) ions adsorbed (mg/g).

In Figure 5, the Morris-Weber curve shows that an initial linear portion may be due to the boundary layer effect (Mohan & Karthikeyan 1997) and a second portion may be due to the intraparticle diffusion effect (Aljeboree *et al.* 2017). The value of the rate constant for the intrapore diffusion K_d was evaluated as 0.5 (g.g min^{-1}) for LS and 5.6 (g.g min^{-1}) for NLS, which gives an indication about the mobility of the Co(II) ions towards the NLS or LS surface.

The order of the adsorption may be examined using the Lagergren equation (Rudzinski & Plazinski 2007):

$$Log(q_e - q) - \log q_e = -K_{ads}\, t/2.303 \tag{6}$$

where q_e is the amount of Co(II) ions adsorbed at equilibrium (mg/g), K_{ads} is the first order rate constant for Co(II) ions adsorption onto sorbent (min^{-1}).

The linear plot of Log ($q_e - q$) vs. t (Figure 6) shows the appropriateness of the above equation and, consequently, the first-order nature of the process involved. The value of K_{ads} was calculated to be 0.027 min^{-1} for LS and 0.04 min^{-1} for NLS.

The amount of the metal which may be introduced into the pores may be investigated by using Bangham's equation

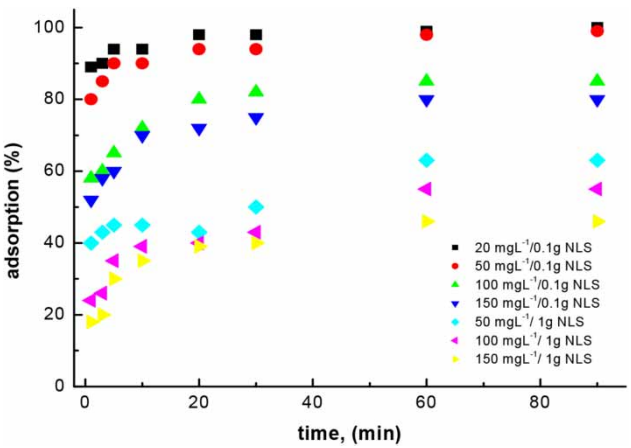

Figure 4 | Influence of stirring time on the adsorption of various concentrations of Co(II) ions by NLS (0.1 g.L^{-1}) and LS (1 g.L^{-1}) at pH 7.

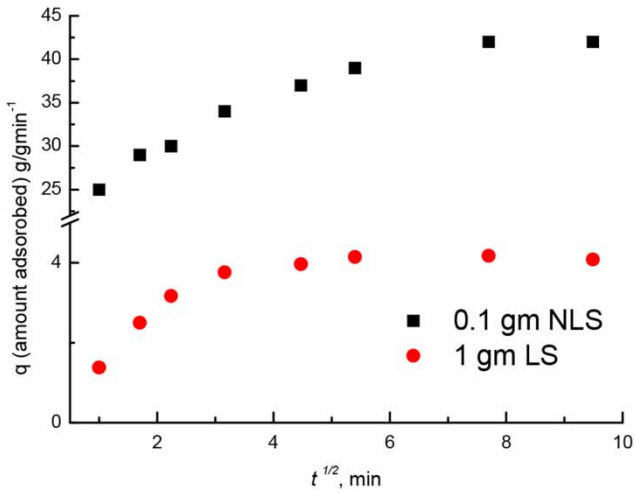

Figure 5 | Plot of the adsorbed amount of Co(II) ions adsorbed onto NLS or LS vs. square root of time at pH 7.

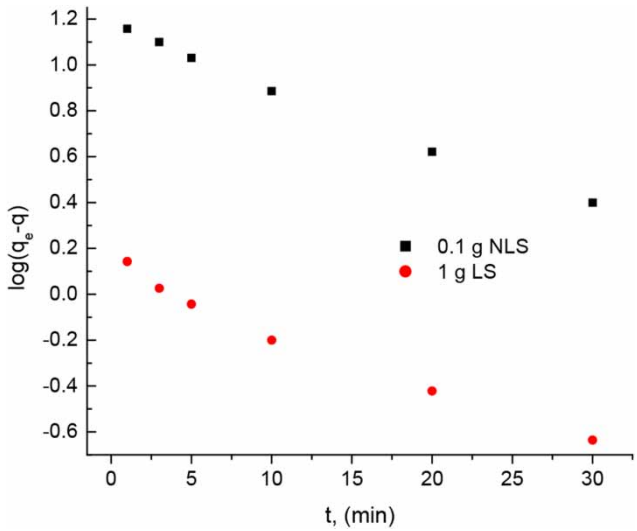

Figure 6 | Plot of log $(q_e - q)$ vs. t stirring time for Co(II) ions adsorption onto NLS or LS.

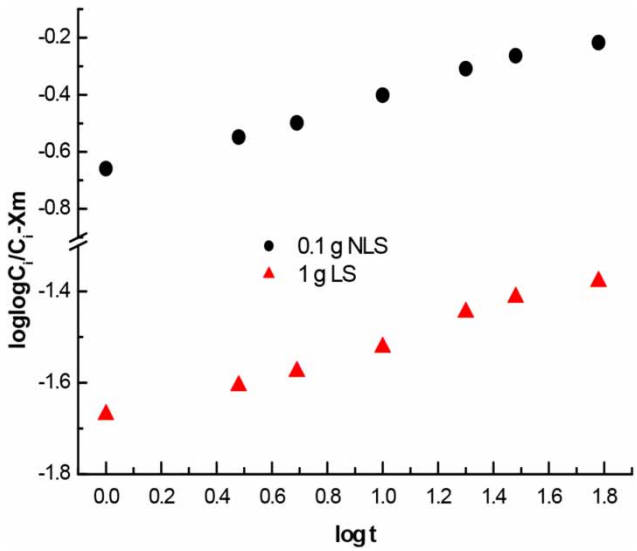

Figure 7 | Plot of log $[C_i/(C_i - q.m)]$ vs. log t for the adsorption of Co(II) ions by NLS or LS at pH 7.

(Mishra 2017):

$$Log\, log[C_i/(C_i - q.m)] = log\,(K_o m/2.303V) + \alpha \log t \quad (7)$$

where K_o is the proportionality constant, and α is Bangham's equation constant.

These results (Figure 7) show that the diffusion of Co(II) ions onto LS pores played a role in the adsorption process (Ali *et al.* 2015). The value of α constants deduced were 0.11 for LS and 0.21 for NLS, respectively, favored to be (less than 1).

Isotherm model

Langmuir isotherm

The Langmuir model is widely used for modeling equilibrium data to indicate the monolarity of the LS surface from the following equation (El-Sheikh *et al.* 2019):

$$C_e/q_e = 1/b.Q_{\max} + (1/Q_{\max}).Ce \quad (8)$$

where b is the monolayer adsorption capacity and relates to the heat of sorption (L.mg^{-1}), Q_{max} is the maximum adsorption capacity (mg.g^{-1}).

Freundlich isotherm

The Freundlich expression is an empirical equation describing sorption to a heterogeneous surface (El-Sheikh *et al.* 2019). The Freundlich equation is presented as:

$$ln\, q_e = ln\, K_f + 1/n\, ln\, Ce \quad (9)$$

where K_f (mol^{1-n} L^n g^{-1}) represents the sorption capacity when metal ion equilibrium concentration equals 1 and n represents the degree of dependence of sorption with equilibrium concentration. Favorable adsorption was demonstrated by the fact that the value of n is greater than unity.

Dubinin–Radushkevich isotherm

The Dubinin–Radushkevich (D-R) isotherm is more general than the Langmuir, because it does not assume a

Table 1 | Calculated parameters of Langmuir, Freundlich, and D-R models for adsorption of Co(II) onto NLS and LS

Langmuir Adsorbent	***b* (L.mg^{-1})**	***Q_{max}*(mg.g^{-1})**	***R^2***
NLS	0.011	60.0	0.997
LS	0.045	17.1	0.988
Freundlich Adsorbent	***K_f*(mol^{n-1} L^n g^{-1})**	***N***	***R^2***
NLS	36.3	3.1	0.998
LS	1.3	1.2	0.979
D-R model Adsorbent	***E* (kJ mol^{-1})**	***$q_{(D\text{-}R)}$* (mg.g^{-1})**	***R^2***
NLS	7.8	134.3	0.995
LS	7.6	40.4	0.968

Table 2 | Thermodynamic data for the adsorption of 50 mgL^{-1} Co(II) ions onto (0.1 g) of NLS and (1 g of LS)

Adsorbent	T(K)	lnK_d	ΔG^o(kJ.mol^{-1})	ΔH^o(kJ.mol^{-1})	ΔS^o(J.mol^{-1}.K^{-1})
NLS	288	7.6	−18.2	41.6	74.8
	298	8.2	−20.5		
	303	8.4	−21.2		
	313	8.5	−22.2		
	323	8.8	−23.7		
LS	288	2.9	−6.9	20.8	33.3
	298	3.5	−8.7		
	303	3.6	−9.1		
	313	3.7	−9.6		
	323	3.8	−10.4		

homogeneous surface or constant sorption potential. In general, the model is compatible between Gaussian energy distribution and adsorption processes on a heterogeneous surface. The D-R equation is expressed as (Özcan *et al.* 2006):

$$ln\, q = ln\, q_{(D-R)} - \beta\varepsilon^2 \tag{10}$$

$$\varepsilon = RT\, ln(1 + 1/Ce) \tag{11}$$

where $q_{(D\text{-}R)}$ is the theortical adsorption capacity ($mg.g^{-1}$); β is the activity coefficient related to mean sorption energy ($mol^2\ kJ^{-2}$); ε is the Polanyi potential; R is the ideal gas constant ($0.008314\ kJ\ mol^{-1}\ K^{-1}$) and T is the absolute temperature in Kelvin (K). E ($kJ\ mol^{-1}$) is defined as the free energy change required to transfer 1 mol of ions from solution to the solid surfaces, which equals:

$$E = 1/(2\beta)^{1/2} \tag{12}$$

The magnitude of E is useful for estimating the type of sorption reaction. If E is in the range of 8–16 $kJ\ mol^{-1}$, the sorption is governed by chemical ion-exchange. In the case of $E < 8\ kJ\ mol^{-1}$, physical forces may affect the sorption. On the other hand, sorption may be dominated by particle diffusion if $E > 16\ kJ\ mol^{-1}$ (Sari *et al.* 2007).

From the results of D-R model simulation (Table 1), E value is 7.6 $kJ\ mol^{-1}$ for LS and 7.8 $kJ\ mol^{-1}$ for NLS, indicating that sorption is governed by chemical ion-exchange according to the theory of the D-R model or sorption may be considered as physical-chemical adsorption (Özcan *et al.* 2006).

Thermodynamic parameters

In order to investigate the effect of temperature on the adsorption of Co(II) ions onto LS, the distribution coefficient, K_d ($L.g^{-1}$), was calculated at the temperatures 288, 298, 313, and 323 K (Table 2) by using Equation (13).

Thermodynamic parameters, the enthalpy change (ΔH^o) and the entropy change (ΔS^o), were calculated from the slope and intercept of the plot of ln K_d against 1/T, respectively (Qadeer & Hanif 1994; Bereket *et al.* 1997; Tahir & Rauf 2003; Ho 2004; Klapiszewski *et al.* 2017):

$$lnK_d = \Delta S^o/R - \Delta H^o/RT \tag{13}$$

The other thermodynamic parameter, Gibbs free energy (ΔG^o) was calculated by:

$$\Delta Go = -RT\, ln\, K_d \tag{14}$$

where R is the universal gas constant ($8.314\ Jmol^{-1}\ K^{-1}$) and T is the temperature (K).

The K_d value increases with increasing temperature revealing the adsorption of metals onto LS to be endothermic.

Table 3 | Adsorption performance for the adsorption of Co(II) onto different adsorbents

Adsorbent	q_e(mg/g)	Reference
Activated carbon	9.93	Kasaini *et al.* (2013)
Carboxy methyl chitosan bed	29.5	Luo *et al.* (2018)
Adsorption of α-C_2SH	14.0	Niuniavaite *et al.* (2018)
Limestone	17.1	This study
Nanolimestone	60.0	This study

Table 4 | Recovery of Co(II) ions added to various natural water samples of pH 7 using (0.9 g L^{-1}) NLS and LS

		NLS			LS		
Sample (location)	**Added Co^{3+} (mg L^{-1})**	**Adsorbed (mg L^{-1})[a]**	**% (Recovery)[b]**	**% R^2**	**Adsorbed (mg L^{-1})[a]**	**% (Recovery)[b]**	**% R^2**
Tap water (our laboratory)	10.0	9.98	99.8	0.994	9.23	92.3	0.995
	15.0	14.84	98.9	0.988	12.53	83.5	0.984
Nile water (Mansoura City)	10.0	9.96	99.6	0.997	8.74	87.4	0.964
	15.0	14.76	98.4	0.987	13.66	91.1	0.947
Sea water (Gamasah)	10.0	9.93	99.3	0.995	6.99	69.9	0.988
	15.0	14.51	93.6	0.965	12.63	84.2	0.956
Underground water (Salaka)	10.0	9.80	98.0	0.981	8.95	89.5	0.977
	15.0	14.32	95.5	0.981	13.65	91.0	0.997
Lake water (El-Manzala)	10.0	9.88	98.8	0.957	7.98	79.8	0.995
	15.0	14.75	98.3	0.969	12.55	83.7	0.947

[a]The mean of five experiments.
[b]Calculated for five experiments.

Thermodynamic parameters, the enthalpy change (ΔH^o) and the entropy change (ΔS^o), were calculated from the slope and intercept of Equation (13).

The other thermodynamic parameter, Gibbs free energy (ΔG^o) was calculated by Equation (14). For the enthalpy change, the positive ΔH^o showed that the adsorption of Co(II) onto both sorbents is endothermic. For the entropy change (ΔS^o), the positive sign means that the adsorption of Co(II) ions onto both sorbents is a random reaction. Also, the negative sign of the ΔG^o indicates that the adsorption of Co(II) onto both sorbents is feasible and spontaneous thermodyamically. In addition, the reaction proceeded physically, and these results were in good agreement with that obtained from the D-R isotherm.

Table 3 shows the performance for the adsorption of Co(II) onto different adsorbents.

APPLICATION

To investigate the applicability of the recommended procedure, a series of experiments was performed to recover 10.0 and 15 mg L^{-1} of Co(II) ions added to aqueous and some natural water samples using LS and NLS. The adsorption experiments were carried out using clear, filtered, and uncontaminated sample solutions after adjusting their pH values to 7. The results obtained are listed in Table 4; the lower recovery values of Co(II) ions from some water samples could be enhanced by increasing the NLS or LS dose.

CONCLUSION

The experimental results indicate that NLS and LS can be successfully used for the adsorption of Co(II) ions from aqueous solutions. The equilibrium data well followed the Langmuir and Freundlich models. The value of mean sorption energy, E, obtained from the D-R isotherm indicated that the adsorption of the metals on the LS was feasible and spontaneous. The negative ΔH^o value depicted that the adsorption of Co(II) onto LS was an endothermic process, and the increase in K_d values with increasing temperature also supported this conception. The positive ΔS^o values revealed the randomness of the adsorbed system. On the basis of all results, it can be calculated that limestone (LS) can effectively be used for the removal of cobalt metal cations from different water systems using adsorption method. The nanolimestone presents the major advantage of providing low cost recovery processes making it useful for use in water purification.

ACKNOWLEDGEMENTS

The authors extend their appreciation to the Deanship of Scientific Research at King Khalid University for funding

this work through Group Research Project under grant number (R.G.P.1/35/38).

REFERENCES

Abdel-Raouf, M. S. & Abdul-Raheim, A. R. M. 2017 Removal of heavy metals from industrial waste water by biomass-based materials: a review. *Journal of Pollution Effects & Control* **5** (1), 1–13.

Ali, S. W., Mirza, M. L., Bhatti, T. M., Naeem, K. & Din, M. I. 2015 Dispersion of iron nanoparticles by polymer-based hybrid material for reduction of hexavalent chromium. *Journal of Nanomaterials* **16** (1), 403.

Aliabdo, A. A., Elmoaty, A. E. M. A. & Auda, E. M. 2014 Reuse of waste marble dust in the production of cement and concrete. *Construction and Bulding Materials* **50**, 28–41.

Aljeboree, A. M., Alshirifi, A. N. & Alkaim, A. F. 2017 Kinetics and equilibrium study for the adsorption of textile dyes on coconut shell activated carbon. *Arabian Journal of Chemistry* **10**, 3381–3393.

Al-Qodah, Z. 2006 Biosorption of heavy metal ions from aqueous solutions by activated sludge. *Desalination* **196** (1–3), 164–176.

Apak, R., Güçlü, K. & Turgut, M. H. 1998 Modeling of copper (II), cadmium (II), and lead (II) adsorption on red mud. *Journal of Colloid and Interface Science* **203** (1), 122–130.

Aziz, H. A., Adlan, M. N. & Ariffin, K. S. 2008 Heavy metals (Cd, Pb, Zn, Ni, Cu and Cr (III)) removal from water in Malaysia: post treatment by high quality limestone. *Bioresource Technology* **99** (6), 1578–1583.

Badruzzaman, M., Westerhoff, P. & Knappe, D. R. 2004 Intraparticle diffusion and adsorption of arsenate onto granular ferric hydroxide (GFH). *Water Research* **38** (18), 4002–4012.

Bates, R. L. & Jackson, J. A. 1980 *Glossary of Geology*, 2nd edn. American Geological Institute, Falls Church, VA, USA.

Bereket, G., Arog, A. Z. & Özel, M. Z. 1997 Removal of Pb (II), Cd (II), Cu (II), and Zn (II) from aqueous solutions by adsorption on bentonite. *Journal of Colloid and Interface Science* **187** (2), 338–343.

Camel, V. 2003 Solid phase extraction of trace elements. *Spectrochimica Acta Part B: Atomic Spectroscopy* **58** (7), 1177–1233.

Cherniak, D. J. 1997 An experimental study of strontium and lead diffusion in calcite, and implications for carbonate diagenesis and metamorphism. *Geochimica et Cosmochimica Acta* **61** (19), 4173–4179.

Doğan, M., Alkan, M., Türkyilmaz, A. & Özdemir, Y. 2004 Kinetics and mechanism of removal of methylene blue by adsorption onto perlite. *Journal of Hazardous Materials* **109** (1–3), 141–148.

Elkady, M., Hassan, H. S. & Hashim, A. 2016 Immobilization of magnetic nanoparticles onto amine-modified nano-silica gel for copper ions remediation. *Materials* **9** (6), 460.

El-Sheikh, A. H., Shudayfat, A. M. & Fasfous, I. I. 2019 Preparation of magnetic biosorbents based on cypress wood that was pretreated by heating or TiO2 deposition. *Industrial Crops and Products* **129**, 105–113.

Ghazy, S. E. & Ragab, A. H. 2007 Removal of lead from water samples by sorption onto powdered limestone. *Separation Science and Technology* **42** (3), 653–667.

Gode, F. & Pehlivan, E. 2003 A comparative study of two chelating ion-exchange resins for the removal of chromium (III) from aqueous solution. *Journal of Hazardous Materials* **100** (1–3), 231–243.

Hariharan, M., Varghese, N., Cherian, A. B. & Paul, J. 2014 Synthesis and characterisation of $CaCO_3$ (Calcite) nano particles from cockle shells using chitosan as precursor. *International Journal of Scientific and Research Publications* **4** (10), 1–5.

Ho, Y. S. 2004 Selection of optimum sorption isotherm. *Carbon* **42** (10), 2115–2116.

Hussain, A. & Ivanovic, M. 2015 Electronics, Communications and Networks IV. In: *Proceedings of the 4th International Conference on Electronics, Communications and Networks (CECNET IV)*, 12–15 December 2014, Beijing, China.

Kasaini, H., Kekana, P. T., Saghti, A. A. & Bolton, K. 2013 Adsorption characteristics of cobalt and nickel on oxalate-treated activated carbons in sulphate media. *World Academy of Science, Engineering and Technology* **76**, 707–721.

Kim, M. S., Hong, K. M. & Chung, J. G. 2003 Removal of Cu (II) from aqueous solutions by adsorption process with anatase-type titanium dioxide. *Water Research* **37** (14), 3524–3529.

Klapiszewski, Ł., Siwińska-Stefańska, K. & Kołodyńska, D. 2017 Development of lignin based multifunctional hybrid materials for Cu (II) and Cd (II) removal from the aqueous system. *Chemical Engineering Journal* **330**, 518–530.

Leyssens, L., Vinck, B., Van Der Straeten, C., Wuyts, F. & Maes, L. 2017 Cobalt toxicity in humans – A review of the potential sources and systemic health effects. *Toxicology* **387**, 43–56.

Luo, W., Bai, Z. & Zhu, Y. 2018 Fast removal of Co (ii) from aqueous solution using porous carboxymethyl chitosan beads and its adsorption mechanism. *RSC Advances* **8** (24), 13370–13387.

Mishra, V. 2017 Modeling of batch sorber system: kinetic, mechanistic, and thermodynamic modeling. *Applied Water Science* **7** (6), 3173–3180.

Mohammadi, A. & Aliakbarzadeh Karimi, A. 2017 Methylene blue removal using surface-modified TiO_2 nanoparticles: a comparative study on adsorption and photocatalytic degradation. *Journal of Water and Environmental Nanotechnology* **2** (2), 118–128.

Mohan, S. V. & Karthikeyan, J. 1997 Removal of lignin and tannin colour from aqueous solution by adsorption onto activated charcoal. *Environmental Pollution* **97** (1–2), 183–187.

Ndifor-Angwafor, N. G., Tiotsop, I. K., Tchuifon, D. T. & Ngakou, C. 2017 Biosorption of amaranth red in aqueous solution onto treated and untreated lignocellulosic materials (pineapple peelings and coconut shells). *Journal of Materials and Environmental Science* **8** (12), 4199–4212.

Niuniavaite, D., Baltakys, K. & Dambrauskas, T. 2018 The adsorption kinetic parameters of Co^{2+} ions by α-C_2SH. *Buildings* **8**, 10.

Özcan, A., Öncü, E. M. & Özcan, A. S. 2006 Kinetics, isotherm and thermodynamic studies of adsorption of Acid Blue 193 from aqueous solutions onto natural sepiolite. *Colloids and Surfaces A: Physicochemical and Engineering Aspects* **277** (1–3), 90–97.

Payne, L. R. 1977 The hazards of cobalt. *Occupational Medicine* **27** (1), 20–25.

Qadeer, R. & Hanif, J. 1994 Kinetics of uranium (VI) ions adsorption on activated charcoal from aqueous solutions. *Radiochimica Acta* **65** (4), 259–264.

Quintelas, C., Rocha, Z., Silva, B., Fonseca, B., Figueiredo, H. & Tavares, T. 2009 Removal of Cd (II), Cr (VI), Fe (III) and Ni (II) from aqueous solutions by an E. coli biofilm supported on kaolin. *Chemical Engineering Journal* **149** (1–3), 319–324.

Reshetnyak, E., Ivchenko, N. & Nikitina, N. 2012 Photometric determination of aqueous cobalt (II), nickel (II), copper (II) and iron (III) with 1-nitroso-2-naphthol-3, 6-disulfonic acid disodium salt in gelatin films. *Open Chemistry* **10** (5), 1617–1623.

Romero-Gonzalez, J., Peralta-Videa, J. R., Rodriguez, E., Delgado, M. & Gardea-Torresdey, J. L. 2006 Potential of Agave lechuguilla biomass for Cr (III) removal from aqueous solutions: thermodynamic studies. *Bioresource Technology* **97** (1), 178–182.

Rudzinski, W. & Plazinski, W. 2007 Studies of the kinetics of solute adsorption at solid/solution interfaces: on the possibility of distinguishing between the diffusional and the surface reaction kinetic models by studying the pseudo-first-order kinetics. *The Journal of Physical Chemistry C* **111** (41), 15100–15110.

Sapuan, S. M., Pua, F. L., El-Shekeil, Y. A. & AL-Oqla, F. M. 2013 Mechanical properties of soil buried kenaf fibre reinforced thermoplastic polyurethane composites. *Materials & Design* **50**, 467–470.

Sari, A., Tuzen, M. & Soylak, M. 2007 Adsorption of Pb (II) and Cr (III) from aqueous solution on Celtek clay. *Journal of Hazardous Materials* **144** (1–2), 41–46.

Singh, K. K., Senapati, K. K. & Sarma, K. C. 2017 Synthesis of superparamagnetic Fe_3O_4 nanoparticles coated with green tea polyphenols and their use for removal of dye pollutant from aqueous solution. *Journal of Environmental Chemical Engineering* **5** (3), 2214–2221.

Somasundaran, P. & Goddard, E. D. 1979 Electrochemical aspects of adsorption on mineral solids. In: *Modern Aspects of Electrochemistry*. Springer, Boston, MA, USA, pp. 207–250.

Sun, S. & Wang, A. 2006 Adsorption properties of carboxymethyl-chitosan and cross-linked carboxymethyl-chitosan resin with Cu (II) as template. *Separation and Purification Technology* **49** (3), 197–204.

Tahir, S. S. & Rauf, N. 2003 Thermodynamic studies of Ni (II) adsorption onto bentonite from aqueous solution. *The Journal of Chemical Thermodynamics* **35** (12), 2003–2009.

First received 2 September 2018; accepted in revised form 31 March 2019. Available online 26 June 2019